Antimony-resistant but not antimony-sensitive *Leishmania donovani* up-regulates host IL-10 to overexpress multidrug-resistant protein 1

Budhaditya Mukherjee[a,1], Rupkatha Mukhopadhyay[a,1], Bijoylaxmi Bannerjee[a], Sayan Chowdhury[a], Sandip Mukherjee[a], Kshudiram Naskar[a], Uday Sankar Allam[b], Dipshikha Chakravortty[b], Shyam Sundar[c], Jean-Claude Dujardin[d,e], and Syamal Roy[a,2]

[a]Infectious Disease and Immunology, Council of Scientific and Industrial Research-Indian Institute of Chemical Biology, Kolkata 700032, India; [b]Microbiology and Cell Biology, Indian Institute of Science, Bangalore 560012, India; [c]Institute of Medical Sciences, Banaras Hindu University, Varanasi 221005, India; [d]Department of Parasitology, Institute of Tropical Medicine, 2000 Antwerp, Belgium; and [e]Department of Biomedical Sciences, University of Antwerp, 2610 Antwerp, Belgium

Edited by Ajit Varki, University of California at San Diego, La Jolla, CA, and accepted by the Editorial Board December 20, 2012 (received for review August 9, 2012)

The molecular mechanism of antimony-resistant *Leishmania donovani* (Sb^RLD)–driven up-regulation of IL-10 and multidrug-resistant protein 1 (MDR1) in infected macrophages (Mϕs) has been investigated. This study showed that both promastigote and amastigote forms of Sb^RLD, but not the antimony-sensitive form of LD, express a unique glycan with *N*-acetylgalactosamine as a terminal sugar. Removal of it either by enzyme treatment or by knocking down the relevant enzyme, galactosyltransferase in Sb^RLD (KD Sb^RLD), compromises the ability to induce the above effects. Infection of Mϕs with KD Sb^RLD enhanced the sensitivity toward antimonials compared with infection with Sb^RLD, and infection of BALB/c mice with KD Sb^RLD caused significantly less organ parasite burden compared with infection induced by Sb^RLD. The innate immune receptor, Toll-like receptor 2/6 heterodimer, is exploited by Sb^RLD to activate ERK and nuclear translocation of NF-κB involving p50/c-Rel leading to IL-10 induction, whereas MDR1 up-regulation is mediated by PI3K/Akt and the JNK pathway. Interestingly both recombinant IL-10 and Sb^RLD up-regulate MDR1 in Mϕ with different time kinetics, where phosphorylation of PI3K was noted at 12 h and 48 h, respectively, but Mϕs derived from IL-$10^{-/-}$ mice are unable to show MDR1 up-regulation on infection with Sb^RLD. Thus, it is very likely that an IL-10 surge is a prerequisite for MDR1 up-regulation. The transcription factor important for IL-10–driven MDR1 up-regulation is c-Fos/c-Jun and not NF-κB, as evident from studies with pharmacological inhibitors and promoter mapping with deletion constructs.

visceral leishmaniasis | antimony resistance | glycoconjugate | antimony efflux

Kala-azar or visceral leishmaniasis, which is caused by the protozoan parasite *Leishmania donovani* (LD), is (re)emerging and spreading worldwide, essentially because of human-made and environmental changes, immunosuppression, and drug resistance (1, 2). To combat the disease, organic pentavalent antimonials were introduced in the Indian subcontinent almost 9 decades ago (3) with dramatic clinical success. However, the toxicity, together with the high treatment failure rate (up to 65%) and the emergence of resistance in Bihar State, India, made the drug obsolete in the Indian subcontinent (4, 5). Nevertheless, it is still used as a first-line treatment in Africa and Latin America (6). Interestingly, 78% of the recent clinical isolates from the hyperendemic zone of Bihar State still showed in vitro resistance to antimonials (7), which might be explained by an increased fitness of the corresponding parasites (8).

Recently, we have demonstrated three unique characteristics of antimony-resistant LD (Sb^RLD). First, it shows a higher concentration of terminal glycoconjugates (*N*-acetylgalactosamine residues) on its surface than antimony-sensitive LD (Sb^SLD) (7). Second, on infection of macrophages (Mϕs), Sb^RLD induces a surge of IL-10 (7, 9). Third, we also observed that Sb^RLD modulates host cells to overexpress the ATP-binding cassette (ABC) transporters multidrug resistance-associated protein 1 (MRP1) and multidrug-resistant protein 1 (MDR1), which results in the efflux of Sb, thus leading to its inability to clear intracellular parasites (7, 10). However, the link between these three observations, as well as the mechanism by which Sb^RLD modulates IL-10 and MDR1 induction from host cells, is still not clear.

In present study, we explore how Sb^RLD and Sb^SLD are being scrutinized by the innate immune cells and the possible bearing of this on the outcome of pathogenesis. We show that Sb^RLD, with its unique glycans, differentially modulates the innate immune receptor, leading to IL-10 induction and subsequent MDR1 up-regulation in host cell. We decipher the cascade of molecular events likely involved in the regulation of these phenomena and propose a model for the interaction between antimonial resistant parasites and their host cell.

Results

Sb^RLD Drives Host Mϕs to Produce IL-10 Through Their Terminal Glycoconjugates. To ascertain the role of terminal *N*-acetylgalactosamine in IL-10 induction, promastigotes of Sb^RLD (BHU575/BHU138) and Sb^SLD (AG83) were subjected to galactosidase treatment. It was observed that the galactosidase-treated Sb^RLD induced significantly less IL-10 production ($P < 0.0001$; two- to 2.5-fold) from Mϕs than its untreated counterpart (Fig. 1*A*). On the other hand, on infection with Sb^SLD, IL-10 production was low and remained unaltered after galactosidase treatment.

Galactosyltransferase (GalT) is the key enzyme that adds up galactose residues on glycans (11). We generated GalT knockdown (KD) Sb^RLD (BHU138 KD/BHU575 KD): A significant decrease in the expression of GalT gene and the surface expression of the *N*-acetylgalactosamine residues was verified by

Author contributions: B.M., R.M., and S.R. designed research; B.M., R.M., B.B., S.C., S.M., K.N., and U.S.A. performed research; D.C. and S.S. contributed new reagents/analytic tools; B.M., R.M., B.B., S.C., J.-C.D., and S.R. analyzed data; and B.M., R.M., and S.R. wrote the paper.

The authors declare no conflict of interest.

This article is a PNAS Direct Submission. A.V. is a guest editor invited by the Editorial Board.

Freely available online through the PNAS open access option.

[1]B.M. and R.M. contributed equally to this work.

[2]To whom correspondence should be addressed. E-mail: sroy@iicb.res.in.

See Author Summary on page 2445 (volume 110, number 7).

This article contains supporting information online at www.pnas.org/lookup/suppl/doi:10.1073/pnas.1213839110/-/DCSupplemental.

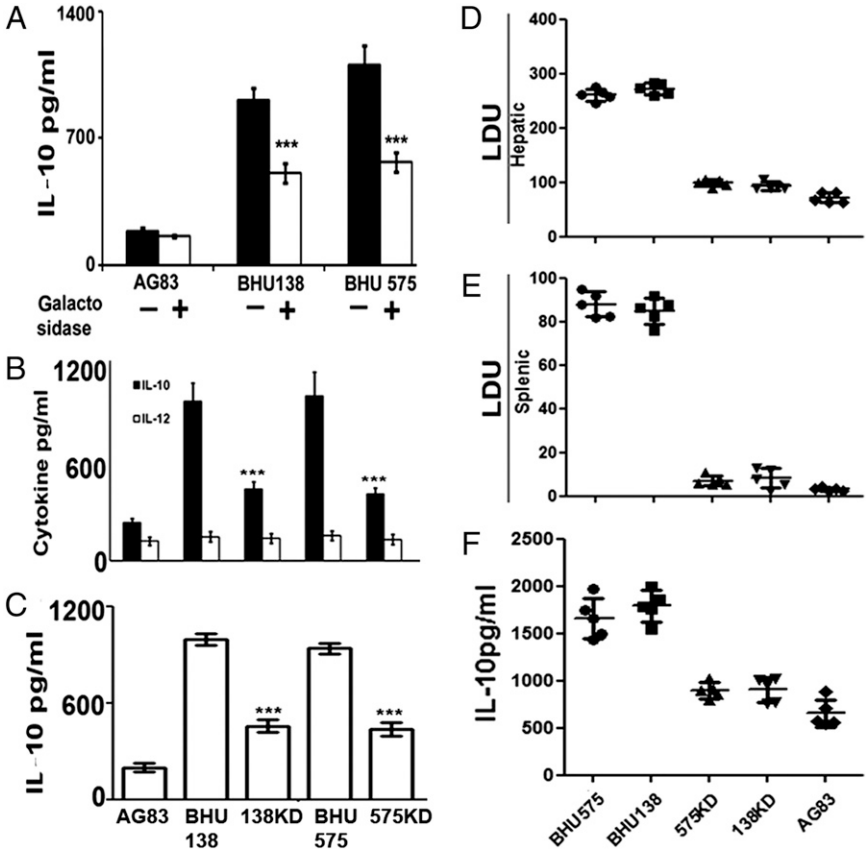

Fig. 1. Surface glycans affect the virulence as well as the IL-10 generation ability of Sb^RLD in host cells. (*A*) Mϕs were cocultured with galactosidase-treated, paraformaldehyde-fixed Sb^SLD (AG83) or Sb^RLD (BHU575/BHU138), or with their untreated counterparts. Unless otherwise stated, all the other experiments were performed at 48 h postinfection. (*B*) Assay of IL-10 and IL-12 in the culture supernatant of Mϕs, infected with either Sb^SLD (AG83) or Sb^RLD (BHU575/BHU138), or with corresponding GalT KD Sb^RLD, by ELISA. (*C*) IL-10 assay in the culture supernatant of Mϕs, treated with the lysates of either Sb^SLD or Sb^RLD, or with corresponding GalT KD Sb^RLD, by ELISA. Hepatic (*D*) and splenic (*E*) parasite burden in infected BALB/c mice in response to infection with either Sb^RLD (BHU575/BHU138) or corresponding GalT KD Sb^RLD (575KD/138KD) or Sb^SLD (AG83) at 3 wk postinfection. (*F*) IL-10 production from splenocytes from mice as in *D* on stimulation with the corresponding SLA. Results in *A*–*C* are presented as the mean ± SD, and results in *D* and *E* are representative of individual samples ± SD. ***$P < 0.001$ (extremely significant). LDU, Leishman-Donovan unit.

RT-PCR and flow cytometry, respectively (Fig. S1 *A* and *B*). Infection of Mϕs with KD Sb^RLD resulted in about two- to threefold lower IL-10 levels ($P < 0.0001$) compared with WT Sb^RLD (Fig. 1*B*). However, the basal level of IL-12 production remained unaltered regardless of the nature of the infecting parasites (Fig. 1*B*).

To verify if the observations described here were stage-specific, we repeated them with animal-derived amastigotes. We found that the amastigotes of Sb^RLD, like the corresponding promastigotes, expressed a significantly higher amount of *N*-acetylgalactosamine residue ($P < 0.0001$; threefold) on their surface (lectin binding study; Fig. S1*C*) and modulated host Mϕs to produce a higher amount of IL-10 ($P < 0.0001$; 2.5- to threefold) compared with Sb^SLD (Fig. S1*D*).

Finally, to determine that the difference in IL-10 induction is due to a quantitative difference in the cell surface glycan rather than intracellular parasite number, Mϕs were treated with the lysate of Sb^RLD, Sb^SLD, or KD Sb^RLD normalized against the number of parasites and also in terms of their protein content, and the resulting IL-10 production was measured. It was observed that Mϕs incubated with Sb^RLD lysate produced significantly higher levels of IL-10 ($P < 0.0001$; two- to threefold) compared with those incubated with either Sb^SLD or KD Sb^RLD (Fig. 1*C*).

Terminal Glycoconjugates Promote the Infectivity of Sb^RLD. To determine the role of terminal glycoconjugates, if any, on in vitro infectivity, Mϕs were infected with Sb^RLD, KD Sb^RLD, or Sb^SLD, and at 24-h time point, the intracellular parasite number was determined. After 24 h, the number of amastigotes per 100 Mϕs ($P < 0.001$; 1.5-fold) was significantly higher on infection with Sb^RLD compared with infection with KD Sb^RLD and Sb^SLD (Fig. S2).

To verify if the same was occurring in an in vivo model, BALB/c mice were infected with the different parasites, and the hepatic as well as splenic parasite load was determined after 3 wk. The parasite load was significantly higher in mice infected with Sb^RLD compared with Sb^SLD or KD Sb^RLD: (*i*) two- to 2.5-fold ratio ($P < 0.001$) in the liver (Fig. 1*D*) and (*ii*) seven- to eight-fold ratio ($P < 0.0001$) in the spleen (Fig. 1*E*). There was significantly higher IL-10 production from the whole splenocytes ($P < 0.001$; 1.5- to twofold) of Sb^RLD-infected mice when stimulated with the corresponding soluble leishmanial antigen (SLA) but not in mice infected with either Sb^SLD or KD Sb^RLD (Fig. 1*F*).

Sb^RLD Exploits Toll-Like Receptor 2 but Not Toll-Like Receptor 4 to Induce IL-10 Production from MΦs. LD infection in THP-1 is reported to cause up-regulation of IL-10 by exploiting Toll-like receptor 2 (TLR2) immune receptors (12). To establish the role of TLR2 in the outcome of Sb^RLD infections, we compared the results obtained with Mϕs derived from C57BL/6 mice, $TLR2^{-/-}$ mice, or C3He/J mice ($TLR4^{-/-}$). On infection with Sb^RLD, we found that the parasite load was two- to threefold lower ($P <$

0.001) in Mϕs from TLR2$^{-/-}$ than in C57BL/6 animals, whereas the difference was not significant with Sb^{S}LD (Fig. S3*A*). In contrast, there was no significant difference in parasite load when Mϕs derived from C57BL/6 and TLR4$^{-/-}$ animals were infected either with Sb^{R}LD or Sb^{S}LD (Fig. S3*A*). In terms of IL-10 production, we found about a threefold ($P < 0.0001$) reduction when TLR2$^{-/-}$ Mϕs were infected with Sb^{R}LD compared with Sb^{S}LD; this was not the case with TLR4$^{-/-}$ Mϕs (Fig. S3*B*). This was not due to a generalized defect, because LPS (an agonist for TLR4)-driven IL-10 production was comparable between C57BL/6-derived and TLR2$^{-/-}$-derived Mϕs (Fig. S3*B*, *Inset*). Furthermore, Sb^{R}LD-mediated IL-10 production was significantly reduced ($P < 0.0001$) in the case of BALB/c Mϕs preincubated with anti-TLR2 and anti-TLR6 Abs, but preincubation with anti-TLR1 Ab had no effect (Fig. S3*C*). The coimmunoprecipitation experiment further revealed the involvement of TLR2/6 in the case of Mϕs infected with Sb^{R}LD (Fig. S3*D*), indicating that heterodimerization of TLR2/6 might be critical for Sb^{R}LD-mediated IL-10 production. Altogether, these findings demonstrate that Sb^{R}LD exploits TLR2/6 heterodimer to induce IL-10 production from Mϕs.

Sb^{R}LD-Driven IL-10 Production Is Dependent on NF-κB. Among the downstream signaling molecules of TLRs, ERK (13), PI3K (14), and NF-κB (15) have been reported to regulate IL-10 production. To identify the most likely signaling molecule in Sb^{R}LD-driven IL-10 production, Mϕs were treated with a series of inhibitors before infection with Sb^{S}LD or Sb^{R}LD. We observed that Sb^{R}LD-driven IL-10 production was largely compromised ($P < 0.0001$; three- to fivefold) in the case of Mϕs pretreated with ERK or NF-κB inhibitor (PD98059, U0126, and BAY110782, respectively; Fig. 2*A*) but not with PI3K (wortmannin), p38 (SB203580), or JNK (SP600125) inhibitor. A similar picture emerged after Western blot analysis: This revealed that infection of Mϕs with Sb^{R}LD (in contrast to Sb^{S}LD) resulted in the activation of ERK1/2 and the degradation of IκB (IκBα, IκBβ, and IκBε) proteins. This corresponds to enhanced IκB kinase α (IKKα) phosphorylation due to increased activity of the upstream IKK complex, as demonstrated from phosphorylation of IKKα/β in Mϕs infected with Sb^{R}LD (Fig. 2*B*). Unlike Sb^{R}LD-mediated infection, there was no phosphorylation of IKKα/β and IκBα when Mϕs were infected with Sb^{S}LD. Also, Sb^{S}LD-induced IL-10 production remained unaffected regardless of the presence or absence of inhibitors. Together, these results demonstrate that Sb^{R}LD-induced IL-10 production by Mϕs is NF-κB dependent.

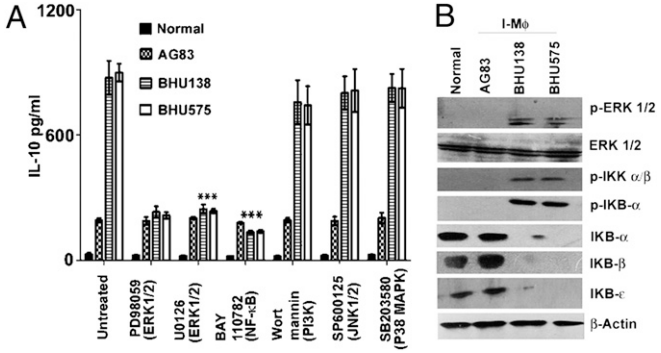

Fig. 2. Sb^{R}LD-driven IL-10 production from Mϕs is dependent on NF-κB. (*A*) IL-10 production from Mϕs infected with either Sb^{S}LD (AG83) or Sb^{R}LD (BHU575/BHU138) in the presence and absence of an array of pharmacological inhibitors (PD98059, U0126, BAY110782, wortmannin, SP600125, and SB203580). (*B*) Western blot analysis of whole-cell lysate derived from the corresponding Mϕ preparation; expression of p-ERK1/2 and ERK1/2 was measured in whole-cell lysates via Western blot analysis using the same membrane. Cytoplasmic IKBα, IKBβ, IKBε, p-IκBα, and p-IKKα/β were detected via Western blot analysis, and the same blot was reprobed for β-actin. Results in *A* are presented as the mean ± SD, and results in *B* are representative of three independent experiments. ***$P < 0.001$ (extremely significant). I-Mϕ, infected Mϕ.

Mapping of IL-10 Promoter. There are three potential NF-κB binding sites at the positions −46/−55, −583/−593, and −917/−927 of IL-10 promoter, defined as site I, site II, and site III, respectively (Fig. S4*A*). To identify the promoter site involved in the Sb^{R}LD-driven IL-10 induction, we transfected Mϕs with several constructs (truncated or not) and assessed luciferase activity on Sb^{R}LD stimulation. The truncated promoter constructs containing site I (−46/−55) and site III (−917/−927) were unable to show enhanced luciferase activity ($P < 0.0001$; three- to fourfold) under Sb^{R}LD stimulation, in contrast to the untruncated construct (Fig. S4*B*). However, the IL-10 promoter construct carrying site I has been reported to show luciferase activity on LPS stimulation, which indicates that a specific stimulus might result in differential modulation of the host promoter (16). Moreover, compared with the WT plasmid carrying the IL-10 promoter construct (1.57 kb), the deleted mutant (Mut) IL-10 promoter construct generated by deleting site II (−583/−593) elicited significantly lower luciferase activity ($P <$ 0.0001; four- to fivefold) in transfected cells when infected with Sb^{R}LD (Fig. S4*C*). This observation indicated that the sequence −583/−593 (site II) is critical for NF-κB–mediated transcriptional activation of the IL-10 gene under Sb^{R}LD stimulation.

Characterization of NF-κB Subunits. To determine the NF-κB subunits involved in IL-10 promoter activity, a ChIP assay was performed. Immunoprecipitation with acetylated H3, p50, c-Rel, and p65 Abs followed by PCR amplification revealed that p50 and c-Rel, but not p65, were bound to site II (−583/−593) when infected with Sb^{R}LD but not with Sb^{S}LD (Fig. 3*A*). This observation was further substantiated by Western blot analysis. There was detectable expression of phosphorylated p50 and c-Rel in the nuclear fraction when Mϕs were infected with Sb^{R}LD but not with Sb^{S}LD, although cytoplasmic expression of whole p50 and c-Rel was almost equivalent on infection with all strains (Fig. 3*B*). Finally, specific binding of NF-κB complexes consisting of p50 and c-Rel subunits to the sequence $^{-583}$GGGGTTTCCT^{-593} (site II) in Mϕs infected with Sb^{R}LD was confirmed with EMSA using murine IL-10 probes containing the WT sequence $^{-583}$GGGGTTTCCT^{-593} (WT mIL-10 probe) or a mutant sequence $^{-583}$CTCTTTTAAT^{-593} (Mut mIL-10 probe) (Fig. 3*C*). Furthermore, supershift analysis with Abs for p50, c-Rel, and p65 revealed that a supershift occurs only in the presence of p50 and c-Rel Abs but not with p65 Ab (Fig. 3*D*). Altogether, these results demonstrate that Sb^{R}LD infection specifically modulates site II (−583/−593) of IL-10 promoter to induce p50/c-Rel binding, thereby initiating IL-10 transcription.

Sb^{R}LD-Induced MDR1 Overexpression Is Dependent on IL-10. To find out the relation, if any, between IL-10 production and overexpression of a host cell's MDR1, Mϕs were incubated with different concentrations of recombinant IL-10 (rIL-10). We found that MDR1 expression occurred in a dose-dependent manner (Fig. S5*A*), whereas an unrelated cytokine like rIL-2 failed to show any effect. In addition, MDR1 expression was significantly reduced in the presence of Ab to IL-10 ($P < 0.001$; threefold) (Fig S5*A*, *Inset*). The link between IL-10 and MDR1 expression was further substantiated using confocal microscopy. We found that incubation with rIL-10 or infection with Sb^{R}LD, but not with Sb^{S}LD, showed enhanced expression of MDR1 (Fig. S5*B*). Altogether, the results indicate a role of IL-10 in host MDR1 overexpression.

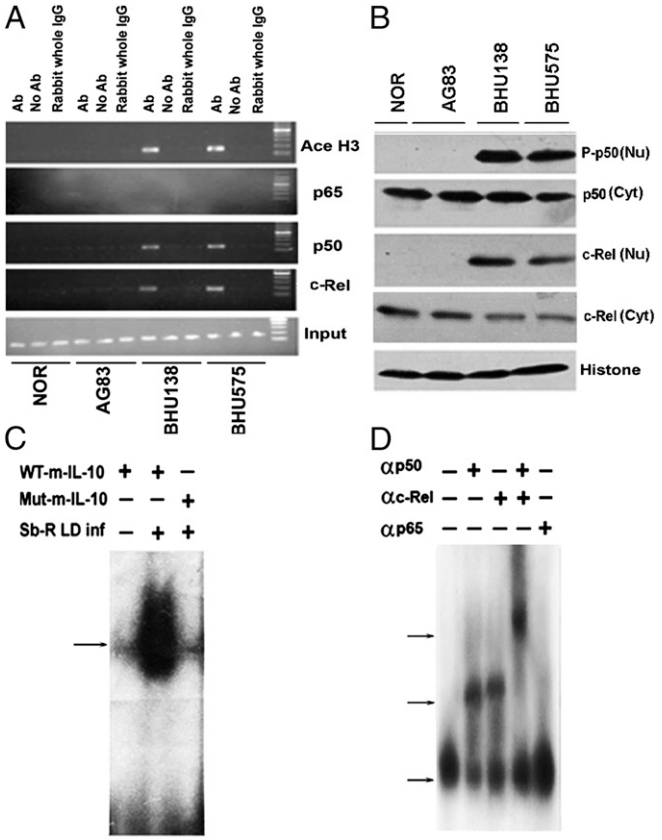

Fig. 3. Sb^RLD activates p50/c-Rel to bind with IL-10 promoter. (*A*) ChIP analysis of IL-10 promoter (−482/−645) with nuclear extract derived from Mϕs infected with Sb^SLD (AG83) or Sb^RLD (BHU575/BHU138) and assessed with Abs to hyperacetylated histone H3 (Ace H3), p65, p50, and c-Rel, followed by PCR amplification. Chromatin immunoprecipitated by whole-rabbit IgG and no Abs was used as a negative control, and input DNA (5%) was used as an internal control. (*B*) Nuclear and cytoplasmic extracts derived from Mϕs infected with either Sb^SLD (AG83) or Sb^RLD (BHU575/BHU138) were used to analyze the expression of phspho-p50 (P-p50) and c-Rel in the nuclear extract (Nu) and the expression of whole p50 and c-Rel in the cytoplasmic extract (Cyt) by Western blot analysis, where histone was used as an internal control. (*C*) Analysis by EMSA of NF-κB DNA binding to IL-10 promoter-specific probes containing a WT NF-κB binding site (WT-m-IL-10 probe) or mutant NF-κB binding site (Mut-m-IL-10 probe). Sb-R LD inf, Sb^RLD infection. (*D*) Characterization of DNA binding of different NF-κB complexes to WT mIL-10 probe by supershift analysis using Abs specific for the indicated NF-κB subunits. Results in *A*–*D* are representative of three independent experiments.

MDR1 as an Effective Efflux Pump. Because our results indicated that the surface glycans of Sb^RLD induce IL-10–mediated MDR1 overexpression in host cells, we wanted to determine the susceptibility of KD Sb^RLD to sodium stibogluconate (SSG). Mϕs were infected with Sb^RLD, Sb^SLD, or KD Sb^RLD, and intracellular parasite number was determined in the presence or absence of SSG. As expected, there was a significant reduction ($P < 0.0001$; five- to sixfold) in intracellular parasite number in Mϕs infected with Sb^SLD in the presence of SSG. Mϕs infected with KD Sb^RLD also showed an increased responsiveness ($P < 0.001$; two- to 2.5-fold) toward SSG compared with Sb^RLD (Fig. S5*C*). Second, using an Rh123 efflux assay, we demonstrated an efflux of Rh123 when Mϕs were infected with Sb^RLD but not with Sb^SLD or KD Sb^RLD (Fig. S5*D*). Moreover, rIL-10 treatment showed a gradual decrease in Rh123 retention in normal Mϕs. In contrast, incubation with an increasing concentration of rIL-2 did not alter Rh123 level (Fig. S5*E*). Altogether, these findings showed that the surface glycans of Sb^RLD may have a role in IL-10–mediated Sb resistance of the parasite in host cells.

IL-10–Dependent MDR1 Up-Regulation Is Independent of NF-κB. Previous reports showed that the MDR1 up-regulation of Mϕs is mediated by the PI3K and Jun kinase pathways (17, 18). To determine the pathway involved in MDR1 up-regulation, pharmacological inhibitors of PI3K, JNK, NF-κB, and ERK were used. From flow cytometric analysis, it was evident that all these pharmacological inhibitors except BAY110782 (inhibitor of NF-κB) and SB204580 (inhibitor of p38MAPK) could significantly abrogate ($P < 0.001$; two- to fourfold) rIL-10–mediated MDR1 overexpression (Fig. S6*A*). To validate this observation, Mϕs were either infected with Sb^RLD (BHU575) or treated directly with rIL-10 and Western blot analysis was performed. As shown here, infection with Sb^RLD induced degradation of IκB proteins, corresponding to enhanced IKKα/β phosphorylation; this was not the case with Mϕs directly treated with rIL-10 (Fig. S6*B*). Therefore, we can conclude that rIL-10–induced MDR1 expression in Mϕs is independent of NF-κB and p38MAPK.

Molecular Events of IL-10–Dependent MDR1 Up-Regulation. To determine signaling molecules eventually leading to MDR1 up-regulation, Mϕs were infected with either Sb^RLD or Sb^SLD or treated with rIL-10 (200 pg/mL) for different periods of time (6, 12, 18, 24, and 48 h). When Mϕs were infected with Sb^RLD, the IL-10 level showed a slight increase at 18 h, peaked at 24 h ($P < 0.0001$; four- to sixfold), and remained unaltered until 48 h (Fig. 4*A*), whereas MDR1 expression continuously increased until reaching a maximum at 48 h ($P < 0.001$; 2.5- to threefold) (Fig. 4*B*). On the other hand, rIL-10 driven MDR1 up-regulation was faster and reached a peak ($P < 0.0001$; 2.5- to threefold) at 12 h posttreatment. Based on this observation, we chose two time points, early (12 h) and late (48 h), for further investigation. Western blot analysis revealed that at 12 h, rIL-10 could induce significantly higher expression of p-PI3K, p-Akt, and p-JNK, whereas Sb^RLD failed to show expression of any of these molecules. It has been reported previously that phosphorylation of JNK leads to activation of different activator protein-1 (AP-1) subunits (19). Interestingly, our result also showed activation of AP-1 (c-Fos and c-Jun; $P < 0.001$) on rIL-10 treatment at 12 h, whereas other AP-1 subunits like Fra-1, Jun B, and Jun D were absent in the nuclear extract irrespective of the nature of the infection or rIL-10 treatment. However, at 48 h, Sb^RLD could significantly up-regulate PI3K/JNK pathway intermediates, which were inhibited ($P < 0.001$) in the presence of neutralizing α-IL-10 (Fig. 4*C*). Finally, to confirm that IL-10 is indeed responsible for MDR1 up-regulation, Mϕs from IL-$10^{-/-}$ mice and their WT counterparts were infected with either Sb^RLD or Sb^SLD for 48 h. Cells were then analyzed for their surface MDR1 status by flow cytometry. Mϕs from IL-$10^{-/-}$ failed to induce MDR1 ($P < 0.0001$; twofold) on infection with Sb^RLD (Fig. 4*D*), although an equivalent amount of IL-12 production was observed from both IL-$10^{-/-}$ and C57BL/6 Mϕs, indicating the direct role of IL-10 in MDR1 up-regulation (Fig. 4*D*, *Inset*). Altogether, these findings showed that in contrast to IL-10 up-regulation, which is dependent on NF-κB, MDR1 overexpression is dependent on the PI3K/JNK pathway.

Characterization of MDR1 Promoter. A potential AP-1 binding site ($^{-123}$TGAGTCA^{-117}, defined as site A) on the murine MDR1 promoter has previously been reported (20) (Fig. 5*A*). To determine whether site A is indeed modulated by IL-10 to induce MDR1, the MDR1 whole-promoter +37/−154 (191 bp, WLpGL3-MDR1) with site A, and the MDR1 truncated promoter +37/−116 (153 bp, trun-pGL3-MDR1) lacking site A were cloned in a pGL3 basic vector and a luciferase assay was performed. Unlike the total promoter construct (191 bp), the

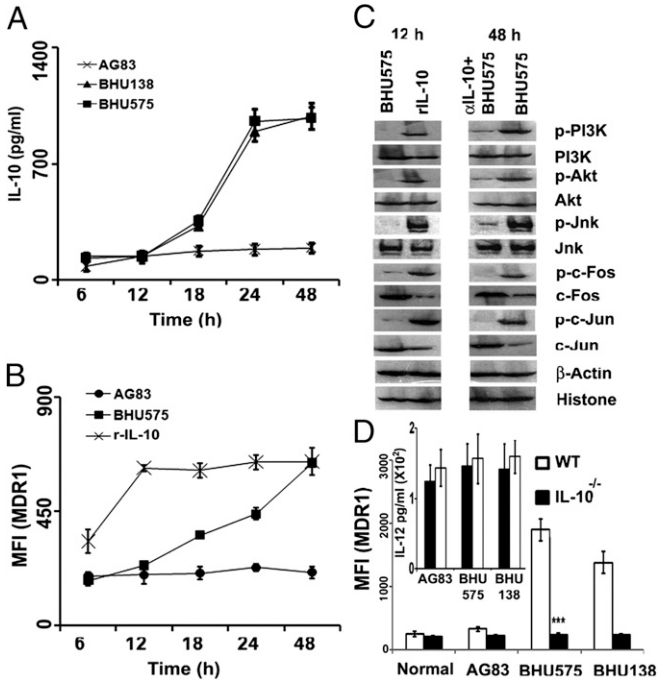

Fig. 4. IL-10 induction by Sb^RLD is a prerequisite for MDR1 up-regulation. (*A*) Kinetics of IL-10 production from infected Mϕs as a function of time. Mϕs were infected with either Sb^RLD (BHU575/BHU138) or Sb^SLD (AG83) for varying periods of time, and IL-10 was measured in the culture supernatant by ELISA. (*B*) Kinetics of MDR1 up-regulation in terms of mean fluorescence intensity (MFI) as a function of time in response to infection with Sb^SLD, Sb^RLD, or rIL-10 (r-IL-10). (*C*) Expression of p-PI3K/PI3K, pAKT/AKT, pJNK/JNK, pc-Fos/c-Fos, and pc-Jun/c-Jun in the cellular extract of Mϕs infected with Sb^RLD (BHU575) at 12 h (early time point) and 48 h (late time point) or treated with rIL-10 (12 h) by Western blot analysis. An identical experiment was performed in the presence of Abs to IL-10 at the 48-h time point. β-actin and histones are used as cytoplasmic and nuclear loading controls, respectively. (*D*) MDR1 expression in Mϕs of IL-$10^{-/-}$ mice or WT C57BL/6 mice on infection with either Sb^SLD (AG83) or Sb^RLD (BHU575/BHU138) in terms of MFI. (*Inset*) Presence of IL-12 in the supernatant from the corresponding infected Mϕ population as in *D* by ELISA. Results in *A*, *B*, and *D* are presented as the mean ± SD, and results in *C* are representative of three independent experiments.

truncated promoter construct (153 bp) failed to show enhanced luciferase activity ($P < 0.001$; four- to fivefold) when stimulated with rIL-10 (200 pg/mL) or Sb^RLD (Fig. 5*B*). From site-directed mutagenesis of site A, it was also observed that compared with the WT plasmid (pGL3-MDR1), the deletion construct (pGL3-MDR1ΔAP1) showed compromised luciferase activity ($P < 0.0001$; 10- to 12-fold) in transfected cells stimulated with rIL-10 (200 pg/mL) (Fig. 5*C*). Furthermore, specific DNA binding of AP-1 to the sequence $^{-123}$TGAGTCA^{-117} of murine MDR1 promoter in response to IL-10 was confirmed via EMSA using murine MDR1 probes containing the WT sequence $^{-123}$TGAGTCA^{-117} (WT MDR1 probe) or the mutant sequence $^{-123}$ACAGTGT^{-117} (Mut MDR1 probe) (Fig. 5*D*) and via supershift analysis (Fig. 5*E*) using Ab for c-Fos, c-Jun, and Fra1. These results demonstrated that cFos/cJun binds specifically with site A of the MDR1 promoter in an IL-10–dependent manner, and thereby causes its overexpression.

Discussion

Research on *Leishmania* drug resistance has focused so far essentially on the parasite itself and the direct molecular adaptations within the parasite (5). Recent studies have shown that *Leishmania* is a master of manipulation of its host cell; consequently, mechanisms of drug resistance should also be addressed at the level of the infected Mϕ. In a previous report, we showed that Sb^RLD could interfere with the signaling system of the Mϕ and counter its oxidative burst (21). In the present study, we explored another domain of the parasite/host cell interaction and deciphered the complex interaction between Sb^RLD-specific parasite surface glycoconjugates, infectivity and IL-10 induction, overexpression of Mϕ MDR1, and efflux of antimonials from the host cell.

We first focused on the terminal glycoconjugates and showed (*i*) that they were overexpressed in amastigote stages, as well as in promastigotes of Sb^RLD, and (*ii*) that this overexpression was correlated with IL-10 induction (Fig. 1 and Fig. S1). Then, two independent experiments (galactosidase treatment and GalT KD Sb^RLD) demonstrated the role of these glycoconjugates in IL-10 induction (Fig. 1 *A* and *B*). The glycan with terminal *N*-acetylgalactosamine is not yet identified, and it is uncertain if it is the molecule solely responsible for IL-10 generation. However, we know already that it is not lipophosphoglycan (LPG; one of the major surface components in *Leishmania*). Indeed, (*a*) unlike LPG, it is expressed both in amastigotes and promastigotes, and

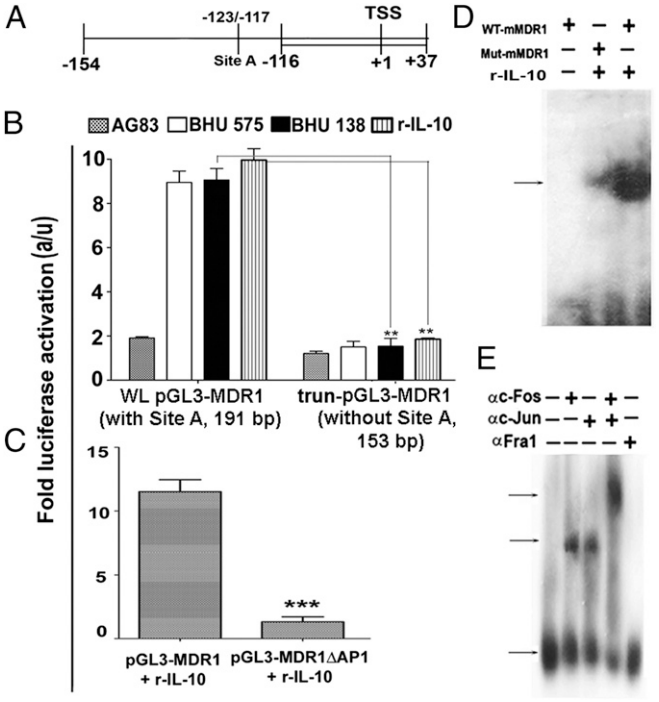

Fig. 5. IL-10–driven MDR1 overexpression is dependent on AP-1. (*A*) Schematic presentation of MDR1 promoter +37/−154 (191 bp) containing an AP-1 binding site (−117/−123) indicated as site A, 191 bp of MDR1 prompter containing site A, and 153 bp of MDR1 promoter (+37/−116) without site A cloned in pGL3-basic vector. TSS, transcription start site. (*B*) Luciferase activity of lysate of RAW264.7 cells transfected with either whole-length construct pGL3-MDR1 promoter (WL, 191 bp) or deletion construct (Δ; trun) of pGL3-MDR1 promoter (lacking site A, 153 bp), followed by infection with either Sb^SLD (AG83) or Sb^RLD (BHU575/BHU138) or treatment with rIL-10. (*C*) Luciferase activity measured in cell lysate of RAW264.7 cells transfected with WT MDR1 promoter construct (191 bp) or Mut MDR1 promoter constructs (−117/−123 deleted) and stimulated with rIL-10 (r-IL-10). a/u, arbitrary unit. (*D*) Nuclear AP-1 DNA binding to MDR1 promoter-specific probes containing a WT AP-1 binding site (WT mMDR1 probe) or a mutant AP-1 binding site (Mut mMDR1 probe) by EMSA. (*E*) DNA binding of different AP-1 complexes to WT mMDR1probe was determined via supershift analysis using Abs specific for indicated AP-1 subunits. Results in *B* and *C* are presented as the mean ± SD, and results in *D* and *E* are representative of three independent experiments.

(*b*) treatment of Mϕs with purified LPG does not induce IL-10 but does induce TNF-α as reported by others (22). Concomitant to IL-10 induction, Sb^RLD also caused higher parasite burdens in vitro and in vivo (Fig. 1 *C* and *D*). There are previous reports that patients who have kala-azar and harbor Sb^RLD show a much higher parasite burden and much greater IL-10 production compared with those harboring Sb^SLD (23, 24). This phenomenon of increased parasite burden in Sb^RLD-mediated infection may also be an attribute of the terminal glycoconjugates, as shown by KD experiments. Interestingly, in vivo parasite loads with Sb^RLD were much higher in the spleen than in the liver, in agreement with previous reports (25, 26). The reason for such a huge difference in the splenic parasite load on infection with Sb^RLD is not clear at the present time. It is tempting to speculate that the surface glycan of Sb^RLD may favor its uptake by the splenic Mϕs. There is a report that the capsular polysaccharide in *Streptococcus pneumonia* interacts with a specific C-type lectin, which favors its uptake by mouse splenocytes (27).

It is not surprising that unlike intracellular Sb^RLD, KD Sb^RLD is more sensitive to SSG-like Sb^SLD because it fails to overexpress host MDR1 (Fig. S5*C*). It is also possible that the unique glycans of Sb^RLD may quench SSG-induced reactive intermediates favoring parasite growth as a consequence of less accumulation of antimonials in Sb^RLD-infected Mϕs due to overexpression of MDR1. This attribute appears to be absent in Mϕs infected with Sb^SLD or KD Sb^RLD, and parasites were killed in response to SSG. It may be recalled that the surface glycocalyx of parasites plays an important role in prevention of SSG-mediated oxidative burst in Mϕs (28).

Second, we focused on the link between antimonial resistance, IL-10 induction, and MDR1 up-regulation. Our study showed that exogenous IL-10 induces up-regulation of MDR1 in a dose-dependent manner, which is inhibited in the presence of α-IL-10 Abs, suggesting that IL-10 may act in an autocrine manner for MDR1 up-regulation (Fig. S5 *A* and *B*). Furthermore, functional assay with Rh123, a fluorescent substrate for MDR1, which is actively effluxed out from Mϕs either infected with Sb^RLD or treated with rIL-10 further supports the notion that Sb^RLD-driven IL-10 is the key factor up-regulating MDR1 and causing efflux of SSG (Fig. S5 *D* and *E*). Kinetic analyses, Western blot studies, and infections of IL-$10^{-/-}$ Mϕs indicated that IL-10 is a prerequisite for MDR1 up-regulation, and this without any direct involvement of Sb^RLD (Fig. 4). It has been reported that MDR1 is responsible for drug resistance in cancer (29). IL-10 overexpression is known to be responsible for chemoresistance in cancer cells (30) or drug unresponsiveness in infected cells (10), but our observation reveals that expression of MDR1 is selectively driven by IL-10.

Third, we characterized the cascade of molecular events likely involved in IL-10 induction and MDR1 up-regulation. Previous reports suggested that activation of ERK is the key step for IL-10 induction (31). Interestingly, infection with Sb^SLD results in the inactivation of host ERK, NF-κB, and JNK, thereby favoring establishment of the parasite (32). In our study, we also did not observe any activation of ERK or NF-κB in Mϕs infected with Sb^SLD, although Sb^RLD activates ERK and nuclear translocation of NF-κB involving p50/c-Rel, leading to IL-10 induction, through interaction with IL-10 promoter site II (−583/−593). Moreover, previous reports have suggested a possible role of PKC in IL-10 induction from Mϕs infected with Sb^SLD (AG83) (33). It is already known that specific stimulations with LPS lead to unique modifications of the IL-10 promoter (15). There is a report that site I (−46/−55) of the IL-10 promoter binds with NF-κB under LPS stimulation (16). Our results (Fig. 3) are in agreement with a previous report stating that the p50/c-Rel activated on infection by *Leishmania major* amastigotes is involved in IL-10 secretion in fresh human monocytes (34).

Previously, it has been shown that TLR2 can differentially recognize peptidoglycans from Gram-positive and Gram-negative bacteria (35). Moreover, recent reports suggest that Sb^SLD (AG83) may deactivate the host TLR2 signaling pathway (36). It is not yet conclusive whether the glycans overexpressed in Sb^RLD directly interact with TLR2. It is possible that the glycans, as well as TLR2, independently contribute to IL-10 up-regulation in the host rather than the glycans interacting directly with TLR2. Earlier reports showed that TLR2 homodimerizes or heterodimerizes with TLR1 or TLR6 (37). Our results suggest that Sb^RLD exploits TLR2/6 heterodimer rather than TLR2/1 heterodimer to induce host IL-10 (Fig. S3). This fits with the previous report that hepatitis C virus induced murine peritoneal Mϕ activation by formation of TLR2/6 heterodimer (38).

There are reports that the PI3K/Akt pathway influences the expression of ABC transporters, such as MRP1 or MDR1 (18). Others have demonstrated that IL-10 activates the PI3K pathway, which results in the activation of Akt (39). With respect to the IL-10–mediated MDR1 up-regulation, we found that it involved (*i*) activation of the PI3K/Akt pathway, leading to activation of JNK and AP-1 but not NF-κB (Fig. 4), and (*ii*) signaling cascade activation of c-Fos and c-jun to translocate and bind to the putative AP-1 binding site on the MDR1 promoter, thus bringing about MDR1 transcription (Fig. 5). Activation of c-Fos and c-Jun to drive MDR1 overproduction in Sb^RLD-infected Mϕs seems unique. Indeed, it has been reported previously that in different species of *Leishmania*, including LD, surface metalloprotease gp63 inactivates all the subunits of the AP-1 transcription factor, because all the subunits, such as c-Fos, c-Jun, Jun B, Jun D, and Fra 1, have putative sites of gp63 cleavage (32). The contrast, compared with our findings, could be explained by experimental differences between the two studies. Contreras et al. (32) focused on the early stage of infection (earliest at 0.5 h and latest at 3 h), whereas we followed it until 48 h. However, the main explanation for the discrepancy likely resides in the unique nature of the Sb^RLD-driven IL-10 induction observed here. This observation probably identifies the expression of AP-1 as a direct effect of IL-10 without any role of input from LD parasites. Mϕs infected with Sb^RLD began to express c-Fos/c-Jun at the 48-h time point, when there is already enough IL-10. However, this is abrogated when Mϕs are preincubated with IL-10 neutralizing Abs, further reinforcing the idea of expression of c-Fos/c-Jun as a direct function of IL-10 (Fig. 4).

This study reports that the Sb^RLD-specific glycans induce IL-10 production from Mϕs, which, in turn, up-regulate host MDR1 and eventually may contribute to drug resistance and increased pathogenicity. It broadens our view of the panel of molecular mechanisms involved in antimonial resistance, highlighting their complementarity. It is remarkable, for instance, that Sb^RLD not only pumps out SbIII, the reduced and active form of the drug, through its own efflux pumps but can manipulate the Mϕ to extrude the prodrug SbV through the MDR1 of the host cell (7). It demonstrates that further studies on drug resistance should definitively not only focus on the parasite but integrate its direct interface, the Mϕ. Finally, it raises concern about the impact of such major molecular adaptations on the outcome of the few available drugs that are implemented in the Indian subcontinent. This is even more concerning, when one is reminded that both Sb and miltefosine exploit the same efflux pump (40). Further work is required to understand if the increasing treatment failure rate of miltefosine in the Indian subcontinent is the consequence of the heritage of the antimonials (41). Our study provides molecular insights as to how Sb^RLD differentially scrutinizes the innate immune machinery of the host, thereby up-regulating IL-10 and subsequently overexpressing MDR1, giving rise to distinct treatment outcomes.

Materials and Methods

Animals. BALB/c mice and golden hamsters (*Mesocricetus auratus*) were maintained and bred under pathogen-free conditions. C57BL/6, TLR2$^{-/-}$, and C3He/J (TLR4$^{-/-}$) mice were obtained from the Indian Institute of Science, and IL-10$^{-/-}$ mice were a kind gift from Gobardhan Das (International Center for Genetic Engineering and Biotechnology, New Delhi, India). Use of both mice and hamsters was approved by the Institutional Animal Ethics Committee of the Indian Institute of Chemical Biology. All animal experiments were performed according to the National Regulatory Guidelines issued by Committee for the Purpose of Supervision of Experiments on Animals, Ministry of Environment and Forest, Government of India.

Parasite Cultures and Maintenance. Sb^{R}LD (MHOM/IN/2009/BHU575/0 and MHOM/IN/2005/BHU138) and Sb^{S}LD (MHOM/IN/83/AG83) (7), maintained in golden hamsters (42), were used for this study. Amastigotes were obtained from the spleen of infected hamsters (43), and they were subsequently transformed into promastigotes and maintained (44).

Cell Culture and Infection. Peritoneal exudate cells, conveniently named Mϕs, were harvested from BALB/c, C57BL/6, TLR2$^{-/-}$, and IL-10$^{-/-}$ mice as described (7). Mϕs were plated, maintained, and infected (1:10 multiplicity of infection) with stationary-phase LD promastigotes. Parasite SLA was prepared as described (44). Parasite lysates from LD promastigotes were generated as described (45), with slight modifications as described in *SI Materials and Methods*.

Treatment. Parasites were treated with galactosidase (0.2 units) and either fixed or left unfixed before infection. Parasite lysates were also used to treat Mϕs. In some experiments, infected Mϕs were treated with 60 μg/mL SSG as described elsewhere (7). In other experiments, Mϕs were treated with various pharmacological inhibitors before infection in serum-free medium. Mϕs were treated with rIL-10 Ab (BD Pharmingen) or with αIL-10 Ab (BD Pharmingen), which was preincubated before infection. In other experiments, TLR2 Ab (10 ng/mL), TLR1 Ab (10 ng/mL), or TLR6 Ab (10 ng/mL) was preincubated with Mϕs for 2 h in serum-free medium before infection. In some experiments, Mϕs were stimulated with either FSL-1 (Invivogen) or Pam3CSK4 (Invivogen), both at a concentration of 10 ng/mL for 24 h. All experiments are described in detail in *SI Materials and Methods*.

Plasmids. The GalT gene construct was generated and cloned in an antisense orientation into the pXG-B2863 vector (a kind gift from S. M. Beverley, University of Washington, Seattle, WA), and it was termed anti-*LdGalT*. The murine IL-10 promoters −17/−1576 (1.57 kb), −17/−292 (275 bp), and −864/−1,138 (274 bp) and the murine MDR1 promoters +37/−154 (191 bp) and +37/−116 (153 bp) were cloned into a pGL3-Basic vector. The Mut IL-10 (with a deletion at NF-κB binding site −583/−593) and Mut MDR1 (with a deletion at AP-1 binding site −117/−123) promoter constructs were generated from the IL-10 (1.57 kb) and MDR1 (191 bp) promoter constructs, respectively, using a QuickChangeII PCR-based site-directed mutagenesis kit (Stratagene) according to the manufacturer's protocol. All experiments are described in detail in *SI Materials and Methods*.

Transfection. Anti-*LdGalT* construct and corresponding empty vector pXG-B2863 were transfected into LD promastigotes by electroporation as described elsewhere (46), and GalT KD parasites (KD Sb^{R}LD) were generated. RAW264.7 cells were grown and transiently transfected with complete IL-10 (1.57 kb) truncated IL-10 (275 or 274 bp), or Mut IL-10 (NF-κB binding site −583/−593), or with complete MDR1 (191 bp), truncated MDR1 (153 bp), or mutant MDR1 (AP-1 binding site −117/−123) promoter constructs. All experiments are described in detail in *SI Materials and Methods*.

RT-PCR Analysis. Total RNA was isolated from GalT KD, WT, or vector control isolates using the Total RNA isolation kit (Roche Biochemicals) according to the manufacturer's protocol. RNA was stored at −70 °C until further use. RT-PCR was performed using specific primers for *LdGalT3* and *GAPDH* following the standard protocol.

Cytokine Measurement. IL-10, IL-12, and TNF-α levels were measured in the supernatant by ELISA (R&D Systems) following the manufacturer's manual.

Dye Uptake and Retention Assay. Rh123 uptake and retention studies were performed fluorometrically as described elsewhere (47), with slight modifications as described in *SI Materials and Methods*.

Immunostaining and Flow Cytometry. The expression levels of *N*-acetylgalactosamine residue in WT as well as KD LD were determined by flow cytometrically using FITC-labeled *Dolichos biflorus* agglutinin and compared with their mannose levels (specific to Con A lectin) (7). The levels of expression of MDR1 in infected or treated Mϕs were determined by immunostaining, followed by flow cytometry (Aria II; Becton Dickinson) and/or confocal microscopy (LSM 510; Carl Zeiss), as described elsewhere (10). Details of the experiment are described in *SI Materials and Methods*.

EMSA. Nuclear extracts were prepared from Mϕs as described elsewhere (9). These extracts were incubated with radiolabeled, double-stranded oligonucleotide probes either for murine IL-10 promoter containing WT or mutant NF-κB binding sites, or for MDR1 promoter containing WT or mutant AP-1 binding sites, respectively. Protein–DNA complexes were separated on acrylamide gels. EMSA was performed using a gel shift assay system (Promega) according to the manufacturer's protocol. Supershift experiments were performed as described in *SI Materials and Methods*.

Western Blot and Coimmunoprecipitation. Cytoplasmic and nuclear protein was prepared, and Western blotting was performed for p50, phospho-p50, and c-Rel (Santa Cruz Biotechnology); pIKKα/β, pIκBα, IκBα, IκBβ, IκBε, pERK1/pERK2 (Thr202/Tyr204), ERK1/ERK2, p65, pPI-3K/PI-3K, pAKT/AKT, pJNK/JNK, pc-Fos/c-Fos, pc-Jun/c-Jun, β-actin, and histone (Cell Signaling Technology) as described in *SI Materials and Methods*. Coimmunoprecipitation was performed as described previously (48) using specific TLR2 Ab (Santa Cruz Biotechnology) or unrelated whole-rabbit IgG (Cell Signaling Technology), and blots were probed with Abs against TLR1 (Santa Cruz Biotechnology) or TLR6 (Santa Cruz Biotechnology).

Reporter Assay. Luciferase activity in cell extracts from infected or treated Mϕs was measured using the Dual Luciferase Reporter kit (Promega) according to the manufacturer's protocols, and the luciferase activity was normalized to the level of the protein content.

ChIP Analysis. ChIP assays were performed on infected Mϕs using a ChIP assay kit (Upstate) following the manufacturer's instructions. Details are provided in *SI Materials and Methods*.

Statistical Variation and Presentation. Each experiment was performed three times, and representative data from one set are presented. Interassay variation was within 10%. Statistical significance between the means of various groups was determined using a two-tailed Student *t* test. Only *P* values below 0.05 were considered to be statistically significant. *P* values <0.001 were considered to be extremely significant (***), *P* values ranging between 0.001 and 0.01 were very significant (**), *P* values ranging between 0.01 and 0.05 were significant (*), and *P* values >0.05 were not significant. Error bars indicate the mean ± SD. Data were analyzed using Prism 5.0 (GraphPad).

ACKNOWLEDGMENTS. We thank Dr. David Sacks, Prof. N. K. Ganguly, and B. Achari for critically reviewing the manuscript. This research was supported by the European Commission-funded Kaladrug-R Project (Health-F3-2008-222895) and the Council of Scientific and Industrial Research, New Delhi.

1. Desjeux P (2004) Leishmaniasis: Current situation and new perspectives. *Comp Immunol Microbiol Infect Dis* 27(5):305–318.
2. Rabello A, Orsini M, Disch J (2003) Leishmania/HIV co-infection in Brazil: An appraisal. *Ann Trop Med Parasitol* 97(Suppl 1):17–28.
3. Brahmachari UN (1989) Chemotherapy of antimonial compounds in kala-azar infection. Part I. By U. N. Brahmachari, 1922. *Indian J Med Res* 89:492–522.
4. Lira R, et al. (1999) Evidence that the high incidence of treatment failures in Indian kala-azar is due to the emergence of antimony-resistant strains of Leishmania donovani. *J Infect Dis* 180(2):564–567.
5. Croft SL, Sundar S, Fairlamb AH (2006) Drug resistance in leishmaniasis. *Clin Microbiol Rev* 19(1):111–126.
6. Chakravarty J, Sundar S (2010) Drug resistance in leishmaniasis. *J Glob Infect Dis* 2(2):167–176.
7. Mukhopadhyay R, et al. (2011) Characterisation of antimony-resistant Leishmania donovani isolates: Biochemical and biophysical studies and interaction with host cells. *Int J Parasitol* 41(13-14):1311–1321.
8. Downing T, et al. (2011) Whole genome sequencing of multiple Leishmania donovani clinical isolates provides insights into population structure and mechanisms of drug resistance. *Genome Res* 21(12):2143–2156.
9. Haldar AK, et al. (2010) Leishmania donovani isolates with antimony-resistant but not -sensitive phenotype inhibit sodium antimony gluconate-induced dendritic cell activation. *PLoS Pathog* 6(5):e1000907.

10. Mookerjee Basu J, et al. (2008) Inhibition of ABC transporters abolishes antimony resistance in Leishmania Infection. *Antimicrob Agents Chemother* 52(3):1080–1093.
11. Dobson DE, et al. (2003) Functional identification of galactosyltransferases (SCGs) required for species-specific modifications of the lipophosphoglycan adhesin controlling Leishmania major-sand fly interactions. *J Biol Chem* 278(18):15523–15531.
12. Chandra D, Naik S (2008) Leishmania donovani infection down-regulates TLR2-stimulated IL-12p40 and activates IL-10 in cells of macrophage/monocytic lineage by modulating MAPK pathways through a contact-dependent mechanism. *Clin Exp Immunol* 154(2):224–234.
13. Feng GJ, et al. (1999) Extracellular signal-related kinase (ERK) and p38 mitogen-activated protein (MAP) kinases differentially regulate the lipopolysaccharide-mediated induction of inducible nitric oxide synthase and IL-12 in macrophages: Leishmania phosphoglycans subvert macrophage IL-12 production by targeting ERK MAP kinase. *J Immunol* 163(12):6403–6412.
14. Martin M, et al. (2003) Role of the phosphatidylinositol 3 kinase-Akt pathway in the regulation of IL-10 and IL-12 by Porphyromonas gingivalis lipopolysaccharide. *J Immunol* 171(2):717–725.
15. Saraiva M, et al. (2005) Identification of a macrophage-specific chromatin signature in the IL-10 locus. *J Immunol* 175(2):1041–1046.
16. Cao S, Zhang X, Edwards JP, Mosser DM (2006) NF-kappaB1 (p50) homodimers differentially regulate pro- and anti-inflammatory cytokines in macrophages. *J Biol Chem* 281(36):26041–26050.
17. Lin CF, Chen CL, Lin YS (2006) Ceramide in apoptotic signaling and anticancer therapy. *Curr Med Chem* 13(14):1609–1616.
18. Misra S, Ghatak S, Toole BP (2005) Regulation of MDR1 expression and drug resistance by a positive feedback loop involving hyaluronan, phosphoinositide 3-kinase, and ErbB2. *J Biol Chem* 280(21):20310–20315.
19. Papachristou DJ, Batistatou A, Sykiotis GP, Varakis I, Papavassiliou AG (2003) Activation of the JNK-AP-1 signal transduction pathway is associated with pathogenesis and progression of human osteosarcomas. *Bone* 32(4):364–371.
20. Hsu SI, et al. (1990) Structural analysis of the mouse mdr1a (P-glycoprotein) promoter reveals the basis for differential transcript heterogeneity in multidrug-resistant J774.2 cells. *Mol Cell Biol* 10(7):3596–3606.
21. Mookerjee Basu J, et al. (2006) Sodium antimony gluconate induces generation of reactive oxygen species and nitric oxide via phosphoinositide 3-kinase and mitogen-activated protein kinase activation in Leishmania donovani-infected macrophages. *Antimicrob Agents Chemother* 50(5):1788–1797.
22. de Veer MJ, et al. (2003) MyD88 is essential for clearance of Leishmania major: Possible role for lipophosphoglycan and Toll-like receptor 2 signaling. *Eur J Immunol* 33(10):2822–2831.
23. Thakur CP, Mitra DK, Narayan S (2003) Skewing of cytokine profiles towards T helper cell type 2 response in visceral leishmaniasis patients unresponsive to sodium antimony gluconate. *Trans R Soc Trop Med Hyg* 97(4):409–412.
24. Verma S, et al. (2010) Quantification of parasite load in clinical samples of leishmaniasis patients: IL-10 level correlates with parasite load in visceral leishmaniasis. *PLoS ONE* 5(4):e10107.
25. Vanaerschot M, et al. (2010) Linking in vitro and in vivo survival of clinical Leishmania donovani strains. *PLoS ONE* 5(8):e12211.
26. Vanaerschot M, et al. (2011) Antimonial resistance in Leishmania donovani is associated with increased in vivo parasite burden. *PLoS ONE* 6(8):e23120.
27. Kang YS, et al. (2004) The C-type lectin SIGN-R1 mediates uptake of the capsular polysaccharide of Streptococcus pneumoniae in the marginal zone of mouse spleen. *Proc Natl Acad Sci USA* 101(1):215–220.
28. Turco SJ, Descoteaux A (1992) The lipophosphoglycan of Leishmania parasites. *Annu Rev Microbiol* 46:65–94.
29. Gottesman MM, Fojo T, Bates SE (2002) Multidrug resistance in cancer: Role of ATP-dependent transporters. *Nat Rev Cancer* 2(1):48–58.
30. Stassi G, et al. (2003) Thyroid cancer resistance to chemotherapeutic drugs via autocrine production of interleukin-4 and interleukin-10. *Cancer Res* 63(20): 6784–6790.
31. Loscher CE, et al. (2005) Conjugated linoleic acid suppresses NF-kappa B activation and IL-12 production in dendritic cells through ERK-mediated IL-10 induction. *J Immunol* 175(8):4990–4998.
32. Contreras I, et al. (2010) Leishmania-induced inactivation of the macrophage transcription factor AP-1 is mediated by the parasite metalloprotease GP63. *PLoS Pathog* 6(10):e1001148.
33. Bhattacharyya S, Ghosh S, Jhonson PL, Bhattacharya SK, Majumdar S (2001) Immunomodulatory role of interleukin-10 in visceral leishmaniasis: Defective activation of protein kinase C-mediated signal transduction events. *Infect Immun* 69(3):1499–1507.
34. Guizani-Tabbane L, Ben-Aissa K, Belghith M, Sassi A, Dellagi K (2004) Leishmania major amastigotes induce p50/c-Rel NF-kappa B transcription factor in human macrophages: Involvement in cytokine synthesis. *Infect Immun* 72(5):2582–2589.
35. Asong J, Wolfert MA, Maiti KK, Miller D, Boons GJ (2009) Binding and Cellular Activation Studies Reveal That Toll-like Receptor 2 Can Differentially Recognize Peptidoglycan from Gram-positive and Gram-negative Bacteria. *J Biol Chem* 284(13): 8643–8653.
36. Srivastav S, Kar S, Chande AG, Mukhopadhyaya R, Das PK (2012) Leishmania donovani exploits host deubiquitinating enzyme A20, a negative regulator of TLR signaling, to subvert host immune response. *J Immunol* 189(2):924–934.
37. Ozinsky A, et al. (2000) The repertoire for pattern recognition of pathogens by the innate immune system is defined by cooperation between toll-like receptors. *Proc Natl Acad Sci USA* 97(25):13766–13771.
38. Chang S, Dolganiuc A, Szabo G (2007) Toll-like receptors 1 and 6 are involved in TLR2-mediated macrophage activation by hepatitis C virus core and NS3 proteins. *J Leukoc Biol* 82(3):479–487.
39. Park HJ, et al. (2011) IL-10 inhibits the starvation induced autophagy in macrophages via class I phosphatidylinositol 3-kinase (PI3K) pathway. *Mol Immunol* 48(4):720–727.
40. Pérez-Victoria JM, et al. (2011) Sitamaquine overcomes ABC-mediated resistance to miltefosine and antimony in Leishmania. *Antimicrob Agents Chemother* 55(8): 3838–3844.
41. Sundar S, et al. (2012) Efficacy of miltefosine in the treatment of visceral leishmaniasis in India after a decade of use. *Clin Infect Dis* 55(4):543–559.
42. Mukhopadhyay S, Sen P, Bhattacharyya S, Majumdar S, Roy S (1999) Immunoprophylaxis and immunotherapy against experimental visceral leishmaniasis. *Vaccine* 17(3):291–300.
43. Hart DT, Vickerman K, Coombs GH (1981) A quick, simple method for purifying Leishmania mexicana amastigotes in large numbers. *Parasitology* 82(Pt 3):345–355.
44. Chakraborty D, et al. (2005) Leishmania donovani affects antigen presentation of macrophage by disrupting lipid rafts. *J Immunol* 175(5):3214–3224.
45. Greig N, Wyllie S, Patterson S, Fairlamb AH (2009) A comparative study of methylglyoxal metabolism in trypanosomatids. *FEBS J* 276(2):376–386.
46. Kapler GM, Coburn CM, Beverley SM (1990) Stable transfection of the human parasite Leishmania major delineates a 30-kilobase region sufficient for extrachromosomal replication and expression. *Mol Cell Biol* 10(3):1084–1094.
47. Kang DI, Kang HK, Gwak HS, Han HK, Lim SJ (2009) Liposome composition is important for retention of liposomal rhodamine in P-glycoprotein-overexpressing cancer cells. *Drug Deliv* 16(5):261–267.
48. Sen S, Roy K, Mukherjee S, Mukhopadhyay R, Roy S (2011) Restoration of IFNγR subunit assembly, IFNγ signaling and parasite clearance in Leishmania donovani infected macrophages: Role of membrane cholesterol. *PLoS Pathog* 7(9):e1002229.